# On the classification of buoyancy-driven chemo-hydrodynamic instabilities of chemical fronts

J. D'Hernoncourt, A. Zebib, and A. De Wit

Citation: Chaos: An Interdisciplinary Journal of Nonlinear Science **17**, 013109 (2007); doi: 10.1063/1.2405129
View online: http://dx.doi.org/10.1063/1.2405129
View Table of Contents: http://scitation.aip.org/content/aip/journal/chaos/17/1?ver=pdfcov
Published by the AIP Publishing

# On the classification of buoyancy-driven chemo-hydrodynamic instabilities of chemical fronts

J. D'Hernoncourt[a)]
*Nonlinear Physical Chemistry Unit and Center for Nonlinear Phenomena and Complex Systems, CP 231, Université Libre de Bruxelles, 1050 Brussels, Belgium*

A. Zebib[b)]
*Mechanical and Aerospace Engineering, Rutgers University, Piscataway, New Jersey 08854-8058*

A. De Wit[c)]
*Nonlinear Physical Chemistry Unit and Center for Nonlinear Phenomena and Complex Systems, CP 231, Université Libre de Bruxelles, 1050 Brussels, Belgium*

(Received 11 August 2006; accepted 15 November 2006; published online 13 February 2007)

Exothermic autocatalytic fronts traveling in the gravity field can be deformed by buoyancy-driven convection due to solutal and thermal contributions to changes in the density of the product versus the reactant solutions. We classify the possible instability mechanisms, such as Rayleigh-Bénard, Rayleigh-Taylor, and double-diffusive mechanisms known to operate in such conditions in a parameter space spanned by the corresponding solutal and thermal Rayleigh numbers. We also discuss a counterintuitive instability leading to buoyancy-driven deformation of statically stable fronts across which a solute-light and hot solution lies on top of a solute-heavy and colder one. The mechanism of this chemically driven instability lies in the coupling of a localized reaction zone and of differential diffusion of heat and mass. Dispersion curves of the various cases are analyzed. A discussion of the possible candidates of autocatalytic reactions and experimental conditions necessary to observe the various instability scenarios is presented. © *2007 American Institute of Physics*. [DOI: 10.1063/1.2405129]

**It is common knowledge that light fluids rise while heavy fluids sink in the gravity field. Buoyant convection due to a hydrodynamic Rayleigh-Taylor instability can therefore be triggered if a heavy solution lies on top of a lighter one. Rayleigh-Bénard convection appears when a fluid is heated from below. Convection can also result from double-diffusive instabilities of a statically stable density stratification if solutal and thermal effects are in competition. However, it is expected that a stratification of a solute-light and hot fluid over a solute-heavy and cold one should always be stable. Here we show that chemical reactions can change this intuitive picture and trigger convection even in cases where concentration and heat both contribute to a stable density stratification. We find that the balance between intrinsic thermal and solutal density gradients initiated by a spatially localized reaction zone and double-diffusive mechanisms are at the origin of a new convective instability of stable density stratifications the mechanism of which is explained by a displaced particle argument. We also classify the stability properties and dispersion curves to be observed for various classes of exothermic chemical fronts depending whether they ascend or descend in the gravity field and whether their solutal and thermal contributions to the density jump across the front are cooperative or antagonistic.**

[a)]Electronic address: jdhernon@ulb.ac.be
[b)]Electronic address: zebib@rutgers.edu
[c)]Electronic address: adewit@ulb.ac.be

## I. INTRODUCTION

The fact that chemical reactions involved in autocatalytic processes can be the source of density gradients able to trigger convection has long been recognized.[1–6] The coupling between nonlinear chemical reactions and diffusion can indeed lead to self-organized interfaces between regions of different compositions and temperatures and hence different densities. In the gravity field, such density stratifications are prone to induce hydrodynamic motions due to either Rayleigh-Taylor, Rayleigh-Bénard, or double-diffusive instabilities. Numerous experimental works have provided clear evidences of such reaction-driven hydrodynamic motions across chemical fronts.[3–31]

To gain insight into such dynamics, it is useful to recall that, across a chemical front, the density difference $\Delta\rho=\rho_p-\rho_r$, where $\rho_p$ and $\rho_r$ stand, respectively, for the density of the product and of the reactant solutions, is a combination of a solutal contribution $\Delta\rho_c$ due to the difference in molar volume of the products versus the reactants and of a thermal part $\Delta\rho_T$ related to the exo- or endothermicity of the reaction. Depending on the relative magnitude and sign of both contributions, various dynamics can be expected as already discussed by Pojman and Epstein.[5] When $\Delta\rho_c$ and $\Delta\rho_T$ are *cooperative*, i.e., have the same sign (which is typically negative as no endothermic autocatalytic reaction is known up to now), solutal and thermal effects combine to transform solute-heavier reactants at room temperature into solute-lighter and hotter products. It is expected that only simple

 

convection can be observed in that case when the front is traveling upwards. Double-diffusive phenomena can become operative when solutal and thermal effects are *antagonistic*, i.e., when $\Delta\rho_c$ and $\Delta\rho_T$ have opposite signs. In that case, both up and down moving fronts can be unstable depending on the relative size of both effects. Numerous modeling and theoretical analyses have been performed on fronts that exhibit simple convection.[32–47] Fewer analytical work have focused on double-diffusive convection of fronts[25,48,49] and it is only recently that heat effects have been shown to allow for new convective instabilities to come into play.[50,51]

A comparison between the stability domains of pure fluids vs those of chemical fronts in the parameter space spanned by the solutal and thermal Rayleigh numbers associated with $\Delta\rho_c$ and $\Delta\rho_T$ shows that chemical reactions profoundly change the stability properties.[51] In particular, a new chemically driven instability can deform chemical fronts even when both solutal and thermal effects are contributing to give a stable density stratification.[50] This instability results from a combination of a localized reaction zone and of differential diffusion of mass and heat.

In this framework, it is the objective of this article to put the classification of chemo-hydrodynamic instabilities of chemical fronts into perspective with regard to experimental conditions. In particular, we classify autocatalytic families of reactions to discuss which dynamics are expected for each of them when they are either ascending or descending in the gravity field. We discuss the dispersion curves and nonlinear dynamics to be expected experimentally in each case comparing with available experimental or numerical data.

The article is therefore organized as follows. In the first section, we review the literature on buoyancy-driven convection around chemical fronts. We next present our theoretical model used to study Rayleigh-Taylor, Rayleigh-Bénard, and double-diffusive instabilities of fronts in Sec. III and define the two important parameters of the problem, which are the solutal and thermal Rayleigh numbers. In Sec. IV, we review the simple convection case, while discussing the properties of the chemically driven mechanism of instability of statically stable fronts in Sec. V. Double-diffusive instabilities are addressed in Sec. VI. Corresponding dispersion curves and nonlinear dynamics are discussed for each case. We end up with conclusions and discussions of possible experimental conditions needed to test our classification.

## II. CLASSIFICATION OF AUTOCATALYTIC REACTIONS

Experiments on buoyancy-driven deformation and acceleration of reaction-diffusion fronts have been performed for quite a long time now. The first experiments were performed in capillary tubes and have addressed the influence of the radius of the tube or of the angle of orientation with respect to gravity on the onset of convection (characterized by one or two convection rolls) and on the speed of the front.[3–21]More recently, experiments in Hele-Shaw cells[21–30] and in a three-dimensional tank[31] have allowed investigation of the dynamics of more extended systems and of the stability of a wider spectrum of instability modes.

Among the literature on such chemo-hydrodynamic deformation of fronts, several autocatalytic families have been studied that can be classified depending on the signs of $\Delta\rho_c$ and $\Delta\rho_T$. An autocatalytic reaction that has been the focus of several experimental studies on convection-driven deformation of fronts is the iodate-arsenous acid (IAA) system that features reactants that are heavier than the products such that $\Delta\rho_c<0$.[6,8,22,23,30,31] This reaction is exothermic as well ($\Delta\rho_T<0$); hence, the solutal and thermal effects are cooperative for the IAA reaction. According to the model of Pojman and Epstein,[5] only simple convection is expected in that case; i.e., only IAA fronts *ascending* the gravity field should be unstable. Indeed, several experimental and theoretical works have focused on characterizing Rayleigh-Taylor induced deformation of *ascending* IAA fronts in capillary tubes,[6,8,32–36] in Hele-Shaw cells,[22,23,30,36–42,45] and in three-dimensional tanks.[31] A similar situation occurs for combustion fronts for which cold liquid fuel reactants are converted into hot gas products.[19,20] Intuitively, it is thus expected that all families of reactions for which solutal and thermal effects have the same sign and are thus reinforcing each other (a class that we will qualify here as "*cooperative*"), the only instability to be expected is of a Rayleigh-Taylor type appearing when the solute-heavier and cooler side of the front lies on top of the solute-lighter and hotter one in the gravity field. As all autocatalytic reactions have $\Delta\rho_T<0$, only ascending fronts are thus thought to be unstable, and indeed most experimental fingering of reactions belonging to the cooperative case have up to now been studied focusing on ascending fronts.

Let us mention here that unstable descending fronts have been observed in both the iodide-nitric acid[21] and iodate-sulfite[11] reactions belonging to this cooperative family wherein both $\Delta\rho_c<0$ and $\Delta\rho_T<0$. In each case, the authors have shown that this unexpected instability could be explained in terms of a solutal double-diffusive instability involving chemical species with different molecular coefficients. They argue that the thermal effects are almost negligible due to the small temperature changes ($\leq 1$ K) associated with the small concentrations used.[11,21] Recently, a theoretical study of the influence of heat losses through the walls of the reactor has shown that the nonmonotonicity of the temperature profile induced by heat losses could destabilize such cooperative-type descending fronts as well.[47] To avoid such complications due to conducting walls, we will assume in the following that the reactor is thermally insulated so that all the heat produced by the reaction results in an adiabatic temperature change.

In the nitric acid-iron(II), chlorite-thiosulfate, chlorite-tetrathionate, chlorate-sulfite, chlorite-thiourea, or bromate-sulfite autocatalytic fronts, the products contract while the reaction is exothermic; hence, $\Delta\rho_c>0$, while $\Delta\rho_T<0$ (see Table I). These fronts, belonging to what we will call the "*antagonist*" class, are typical systems featuring double-diffusive instabilities or also multicomponent convection in the vocabulary of Pojman and Epstein.[5] Both ascending and descending fronts can be unstable due to either Rayleigh-Bénard, Rayleigh-Taylor, or double-diffusive mechanisms depending on the relative values of $\Delta\rho_c$ and $\Delta\rho_T$. A typical example of this family is the chlorite-tetrathionate (CT) reaction, the fingering of which has been extensively

TABLE I. List of autocatalytic reactions for which buoyancy-driven convection due to solutal and thermal density changes across the front have been studied with the relevant reference. A positive $\Delta\rho_c$ means that the products are heavier than the reactants so that isothermal fronts of these reactive systems are buoyantly unstable if they descend in the gravity field. On the contrary, isothermal reactions with a negative $\Delta\rho_c$ feature reactants that are heavier than the products and are thus genuinely unstable in the ascending configuration. All autocatalytic reactions fronts known in the literature are exothermic; i.e., $\Delta\rho_T<0$ (thermal expansion across the front).

| Reaction | $\Delta\rho_c$ | $\Delta\rho_T$ | Reference |
|---|---|---|---|
| Nitric acid-iron(II) | + | − | 3, 4, and 7 |
| Chlorite-thiosulfate | + | − | 4 |
| Chlorite-tetrathionate | + | − | 24–29 |
| Chlorate-sulfite | + | − | 10 |
| Chlorite-thiourea | + | − | 13–16 |
| Bromate-sulfite | + | − | 11 |
| Polymerization front | + | − | 9 and 18 |
| Iodate-arsenous acid | − | − | 6, 8, 22, 23, 30, and 31 |
| Iodide-nitric acid | − | − | 21 |
| Iodate-sulfite | − | − | 11 and 12 |
| Combustion front | − | − | 19 and 20 |

studied.[24–29] For concentrations such that solutal effects dominate the temperature effects, descending fronts are genuinely unstable as the products are heavier than the reactants.[24,26,28,29] At larger concentrations, the exothermicity of the reaction is increased, allowing ascending fronts to be destabilized as well.[25,27,49]

Free radical polymerizations are very exothermic and form polymer products that are more dense than the monomer ($\Delta\rho_c>0$); they fall thus in the same antagonist category.[9,17,18] Various other examples of this family with $\Delta\rho_c>0$ and $\Delta\rho_T<0$ are quoted in Ref. 9. Finally, let us also mention combustion fronts[19,20] that fall generally in the cooperative family as the burned products are typically solute-lighter and hotter than the fuel. The Arrhenius dependence of the kinetic constant on temperature leads however in this case and in the case of strongly exothermic polymerization fronts to possibilities of other instability scenarios that will not be considered here. Table I summarizes different examples with various sign combinations of $\Delta\rho_c$ and $\Delta\rho_T$. Let us now discuss a model that will enable the classification of the various dynamics to be expected for these various systems.

## III. MODEL SYSTEM

Our system is a two-dimensional insulated Hele-Shaw cell of length $L_x$, width $L_y$, and of gap-width $a$ ($a \ll L_x$ and $L_y$), oriented with the gravity field $\underline{g}$ along $\underline{x}$ where the underbar means that the quantity is a vector (see Fig. 1). A reaction-diffusion front is triggered either at the top or the bottom of the cell, yielding a descending or ascending front, respectively, traveling at a reaction-diffusion speed $v$. The system can be described by Darcy's equations (1) and (2) for the velocity field $\underline{u}$ written in the Boussinesq approximation coupled to an advection-reaction-diffusion equation for $C$ and $T$:

$$\nabla \cdot \underline{u} = 0, \tag{1}$$

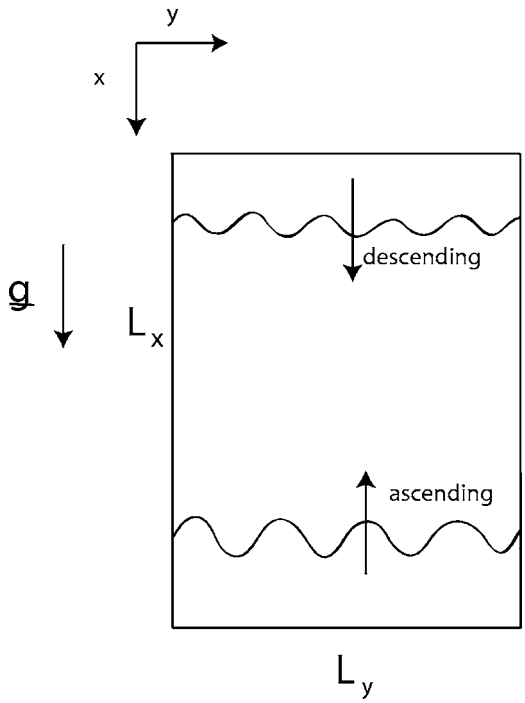


FIG. 1. Sketch of the system.

$$\frac{\mu}{K}\underline{u} = -\nabla p + \rho(C,T)\underline{g}, \tag{2}$$

$$\frac{\partial C}{\partial t} + \underline{u}\cdot\nabla C = D_c\nabla^2 C - f(C), \tag{3}$$

$$\frac{\partial T}{\partial t} + \underline{u}\cdot\nabla T = D_T\nabla^2 T + \frac{\Delta H}{\rho_0 c_p} f(C). \tag{4}$$

The permeability $K=a^2/12$, the viscosity $\mu$, the molecular and thermal diffusion coefficients $D_c$ and $D_T$, respectively, are taken constant, $p$ is the pressure, $c_p$ is the specific heat of water while $\Delta H$ is the heat of the reaction taken here as negative as we consider an exothermic reaction. As a typical nonlinear kinetics able to sustain traveling fronts when coupled to diffusion, we take

$$f(C) = \gamma(C-C_0)(C-C_1)(C+C_2), \tag{5}$$

where $\gamma$ is the kinetic constant, $C_0$ and $C_1$ are the concentrations of the relevant chemical species in the fresh reactant and in the product, respectively (with $C_1>C_0$), while $C_2$ is model dependent. We assume a linear dependence of the density on $C$ and $T$ as

$$\rho(C,T) = \rho_0 + \Delta\rho_c + \Delta\rho_T, \tag{6}$$

where $\rho_0$ is the density of water at room temperature $T_0$, $\Delta\rho_c=-\alpha_c\Delta C$, and $\Delta\rho_T=-\alpha_T\Delta T$, with $\Delta C=C_1-C_0$ and $\Delta T=-\Delta H\Delta C/\rho_0 c_p$ being the concentration and temperature jumps, respectively, across the front. The (positive or negative) solutal and (positive) thermal expansion coefficients are, respectively, $\alpha_c$ and $\alpha_T$. The set of equations is made dimensionless using the following scales: the concentration $C-C_0$ is scaled by $\Delta C$, the temperature $T-T_0$ is scaled by $\Delta T$, the time by $\tau=1/\gamma(\Delta C)^2$, the velocity scale is $U$

$=\sqrt{D_c/\tau}$, and the length scale $l=\sqrt{D_c\tau}$. Incorporating the hydrostatic pressure $\rho_0 g$ in the pressure gradient and considering a descending front, the dimensionless equations (1)–(4) then become

$$\nabla \cdot \underline{u} = 0, \tag{7}$$

$$\underline{u} = -\nabla p + (R_T T + R_c C)\underline{i}_x, \tag{8}$$

$$\frac{\partial C}{\partial t} + \underline{u} \cdot \nabla C = \nabla^2 C + F(C), \tag{9}$$

$$\frac{\partial T}{\partial t} + \underline{u} \cdot \nabla T = \mathrm{Le}\nabla^2 T + F(C), \tag{10}$$

where Le is the Lewis number, i.e., the ratio between the thermal and molecular diffusion coefficients, $\underline{i}_x$ is the unit vector along $x$ aligned with the gravity field for descending fronts and with $F(C)=C(1-C)(C+d)$. As a typical value for the IAA system, for instance, we set $d=0.0021$.[39] The spatial dependence of the basic nondimensional density profile is explicitly obtained as

$$\rho(x) = R_T T(x) + R_c C(x) \tag{11}$$

where the solutal and thermal Rayleigh numbers are defined as

$$R_c = \frac{gK\Delta\rho_c}{\mu U}, \quad R_T = \frac{gK\Delta\rho_T}{\mu U} \tag{12}$$

for a descending front. [Note that the definitions (11) and (12) for a descending exothermic front are the same as in Ref. 50, with $\Delta\rho_c=-\alpha_c\Delta c$ and $\Delta\rho_T=-\alpha_T\Delta T$, but have the opposite sign for an ascending exothermic front as in Ref. 51, where the $x$ axis has been chosen to point upwards to allow for comparison with the classical literature on double diffusion.] Descending cooperative exothermic fronts (such as IAA fronts, for instance) for which $\Delta\rho_c<0$ and $\Delta\rho_T<0$ thus correspond to $R_c$ and $R_T$ both negative [quadrant 3 in the $(R_T,R_c)$ plane of Fig. 2]. Antagonist exothermic fronts (i.e., CT fronts typically) for which $\Delta\rho_c>0$ and $\Delta\rho_T<0$ will feature $R_c>0$ and $R_T<0$ when descending (quadrant 4). For descending fronts, quadrants 1 and 2 (with $R_T>0$ and $R_c$, respectively positive and negative) would then correspond to endothermic reactions. As all autocatalytic chemical systems featuring traveling fronts are known to be exothermic (see Table I), we will here consider only exothermic reactions. Ascending exothermic fronts can easily be studied using similar equations but with $\underline{i}_x$ pointing upwards (as in Ref. 51). This leads us to consider $R_c$ and $R_T$ both positive for ascending cooperative fronts (see Fig. 2). Similarly, $R_T>0$ and $R_c<0$ will correspond to ascending antagonistic fronts with solute-light reactants at room temperature above solute-heavy and hot products.

To analyze the possible convective destabilization of such systems, we perform a linear stability analysis along standard ways.[50,51] In order to do so, we consider the transverse instability of the basic reaction-diffusion front solution of Eqs. (9) and (10) with $\underline{u}=0$ corresponding to the stable products steady state $(C,T)=(1,1)$ invading the unstable reactants steady state $(C,T)=(0,0)$. We introduce perturbations for the concentration, the temperature, the pressure and the velocity of the fluid. We insert these perturbations into the basic state equations (9) and (10) and linearize around the base state. We seek the solutions under normal modes developing the perturbations as $(\delta c,\delta T,\delta p,\delta u,\delta w)=\{\bar{c},\bar{T},\bar{p},\bar{u},\bar{w}\}(z)\exp^{(iky+\sigma t)}$, where $z=x-vt$ is a coordinate moving with the reaction-diffusion speed $v$ of the traveling front and where $k$ and $\sigma$ are the wave number and growth rate of the perturbations, respectively. This allows us to find the dispersion relations giving the growth rate $\sigma$ of the perturbations as a function of their wave number $k$. Instability boundaries are obtained as the parameter values for which the real sign of the largest $\sigma$ becomes positive. Let us now analyze the possible instabilities that can appear in such systems.

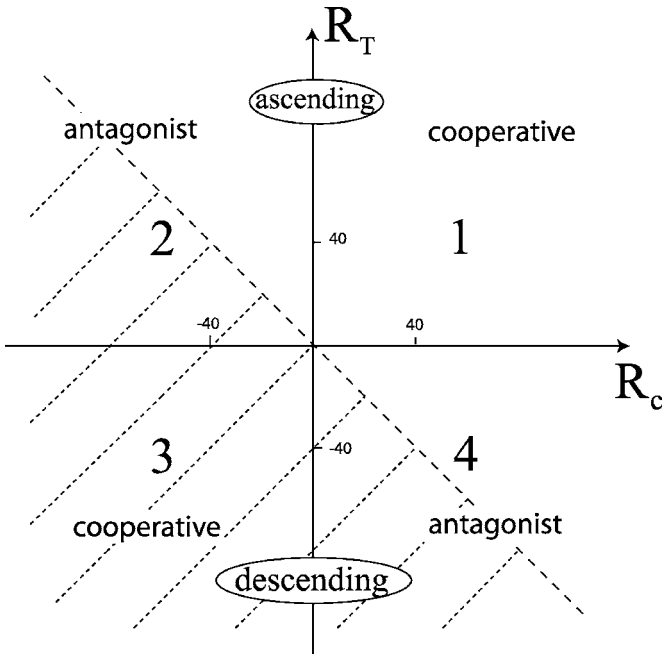


FIG. 2. Stability diagram for Le=1. The shaded area corresponds to the stable zone.

## IV. SIMPLE CONVECTION

The stability diagram in the $(R_T,R_c)$ plane is summarized in Fig. 2 for Le=1. As stated before, quadrant 1, where $R_c>0, R_T>0$ corresponds to ascending cooperative exothermic fronts with a statically unstable density stratification of solute-heavy reactants at room temperature above solute-lighter and hotter products which always leads to instability. In that case, Rayleigh-Taylor fingering is observed characterized by dispersion curves for which the band of unstable modes extends in the range $0\leq k\leq k_c$, where $k_c$ is the critical wave number above which all modes are stable.[23,32–34,39–42] The nonlinear dynamics features one or two convective rolls in capillaries.[8,32,33,35,36] In Hele-Shaw cells, several fingers appear at onset, which then undergo a general coarsening mechanism.[30,38,45] Evolution towards one single self-similar finger[45] or tip splittings[30,45] can then follow, depending on the values of parameters.

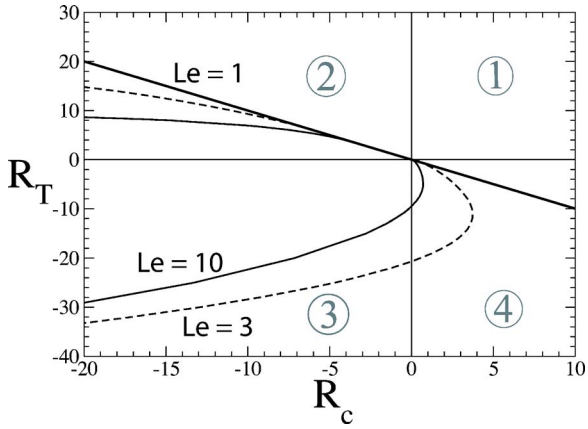


FIG. 3. Stability boundaries for Le=1, 3, and 10. For Le=1, the system is stable below the line $R_T=-R_c$. For Le=3 and 10, the system is stable in the interior of the dashed and full curves, respectively.

Quadrant 3 is always stable for descending cooperative exothermic fronts with Le=1 as it corresponds to a stratification of hot and solute-light products on top of cold and solute-heavy reactants without any possibility of differential diffusion phenomena. In that case, the temperature and concentration profiles both follow the same analytical function.[51] As a consequence, the dashed $R_c=-R_T$ line delineates then the zone of instability (Fig. 2). In quadrant 2 ($R_c<0, R_T>0$), corresponding to ascending antagonistic exothermic fronts, the products are heavier than the reactants, which is a stable situation from the point of view of the solutal component of the density jump. Only reactions which are exothermic enough so that $R_T>|R_c|$ can feature a Rayleigh-Bénard type of instability leading to the observation of thermal plumes.[25,27,49] In quadrant 4 ($R_c>0, R_T<0$); i.e., for descending antagonistic fronts, isothermal fronts are always unstable as the products are heavier. It is only when the reaction is exothermic enough, i.e., when $|R_T|>R_c$ that stabilization of such descending fronts can be achieved as has been shown experimentally for the CT reaction.[27]

## V. INSTABILITY OF STATICALLY STABLE FRONTS

For Le>1, the stability boundaries are modified (see Fig. 3). As already discussed previously,[5,25,49–51] in this case, the temperature profile is then more spread out than the concentration one, and effects due to the differential diffusivity of heat and mass can come into play.

The most striking difference is observed in quadrant 3, which now unexpectedly features a wide zone of instability. When Le>1, we find indeed that, for each negative $R_c$, there is a critical value of negative $R_T$ below which dispersion curves are characterized by a finite band of unstable modes (see Fig. 4). This is intuitively unexpected as the corresponding density profiles in this quadrant are statically stable. Let us indeed plot in Fig. 4 the dimensionless density $\rho$ given by Eq. (11) as a function of $x$ pointing in the direction of propagation of the front. $x\to+\infty$ corresponds to the reactants in which $(c,T)=(0,0)$, while $x\to-\infty$ corresponds to the products in which $(c,T)=(1,1)$, while gravity is aligned towards positive $x$ for descending fronts and towards negative $x$ for ascending ones. We clearly see in Fig. 4 that, in quadrant 3, where $R_T$ and $R_c$ are both negative, the density of the products $\rho_p=R_c+R_T$ is always smaller than the density $\rho_r=0$ of the reactants. Solutal and thermal effects are indeed reinforcing each other ($\Delta\rho_c<0$ and $\Delta\rho_T<0$) to yield across a descending front a density profile increasing monotonically from top to bottom (increasing $x$) when going from the solute-light and hot products towards the solute-heavy reactants at room temperature below them. Intuitively, stability would be expected. Dispersion curves show however destabilization for large enough negative $R_T$. A particle displacement argument provides insight into the chemically driven instability mechanism at play here and which results from a combination of a localized reaction zone and differential diffusion of heat and mass (instability being observed in this quadrant only when Le>1).[50,51] As shown on Fig. 5, let us consider a solute-light and hot particle close to the products region at a concentration $C_a$ and temperature $T_a$, which is displaced downwards into the more effective reaction zone at

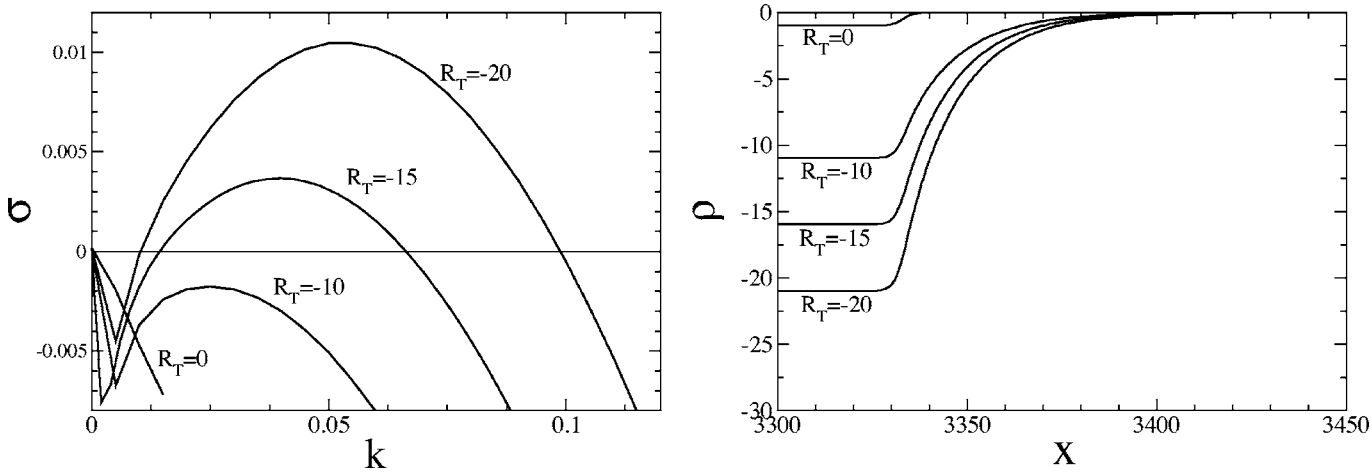


FIG. 4. Dispersion curves and density profiles as a function of $x$ in quadrant 3 ($R_T<0, R_c<0$); i.e., for a cooperative descending exothermic front. The curves are drawn here for Le=10, $R_c=-1$ and various negative $R_T$. Although the density of the product $\rho_p=R_T+R_c$ at the smaller values of $x$ is smaller than the density $\rho_r=0$ of the reactant at larger $x$, the system features a band of unstable modes for $R_T$ below a critical value that depends on $R_c$.

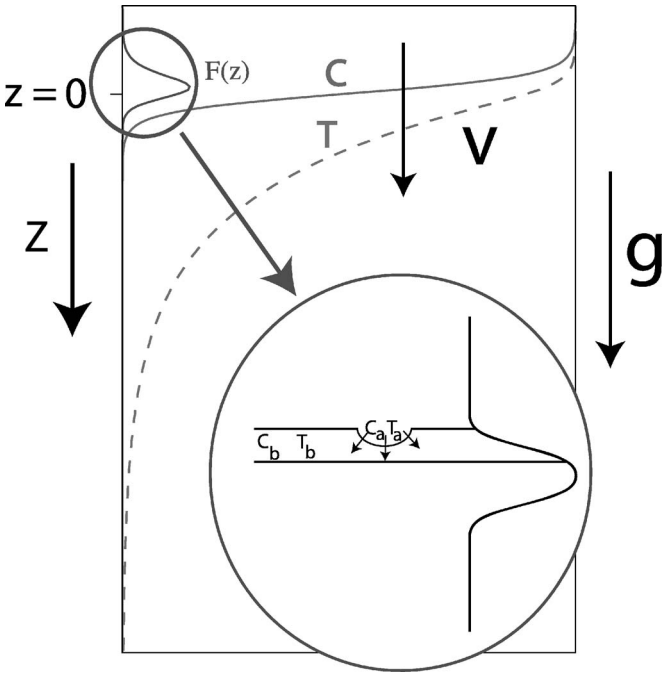


FIG. 5. Concentration $c$, temperature $T$, and chemical reaction rate $F(z)$ profiles for an exothermic downward propagating front. A displaced particle argument allows to understand the chemically driven instability arising in quadrant 3.

larger concentration $C_b$ and temperature $T_b$ in the region where $F(C)$ is increasing. Temperature equilibrates faster than concentration as $\mathrm{Le}>1$. Hence, we obtain a localized zone of composition still close to $C_a$ yet already at the temperature $T_b$ of its surrounding. As $F(C_a)<F(C_b)$, this little particle thus reacts not as much as its immediate neighborhood, thus gaining less heat and concentration (recall the reaction is exothermic) and making it denser. The particle may thus continue to sink driving an instability. We note that, when the particle encounters the lower region where $F(C)$ decreases, the mechanism becomes inverted; in other words, the region of instability localized into the region of increasing $F$ is subdued by the stable zone where $F$ decreases again. As a consequence, the instability leads to eigenfunctions the largest part of which is localized at the back of the traveling chemical fronts and to small fingers of reduced amplitude in the nonlinear regime.[50,51] Concerning the dispersion curves, Fig. 4 shows that for a fixed negative $R_c$, there is a critical negative $R_T$ below which the system becomes unstable. The instability increases with increasing $|R_T|$ as, for a given adiabatic temperature change across the front, the mechanism of this chemically driven instability is correspondingly more efficient. Similarly, the system is more unstable when Le is increased as this reinforces the differential diffusivity helping the onset of the instability. Let us note that the dispersion curves are here of type I[52] with a neutral mode always at zero wave number, stable long-wave modes, and a finite band of unstable modes centered around a critical wave number $k_{\max}$. The transition between the decreasing part and the parabolic-shaped part of the curves is actually smooth and continuous when zooming on the transition zone. Such type I dispersion curves are reminiscent of Turing-type dispersion curves[53–55] and have been shown to yield frozen fingers of fixed wavelength and amplitude close to criticality.[27,49,50]

## VI. MULTICOMPONENT CONVECTION

In quadrant 4, the instability zone is drastically enlarged when $\mathrm{Le}>1$ and extends almost to the whole quadrant except in a small balloon close to $R_c=0$, $|R_T|=0$. As already discussed by Pojman and Epstein[5,7] and Kalliadasis *et al.*,[49] instability can be observed there even when the density profile is statically stable pointing out to the influence of double-diffusive phenomena (also called thermohaline or multicomponent convection).[56–60] Concerning the dispersion curves, in quadrant 4, double-diffusive effects are seen to stabilize long wave modes leading to dispersion curves of type I with a finite band of unstable modes, the zero wave number being marginally unstable.[25,49] Such dispersion curves have been measured experimentally for buoyancy-driven deformation of ascending CT fronts.[25] As a result, the nonlinear dynamics

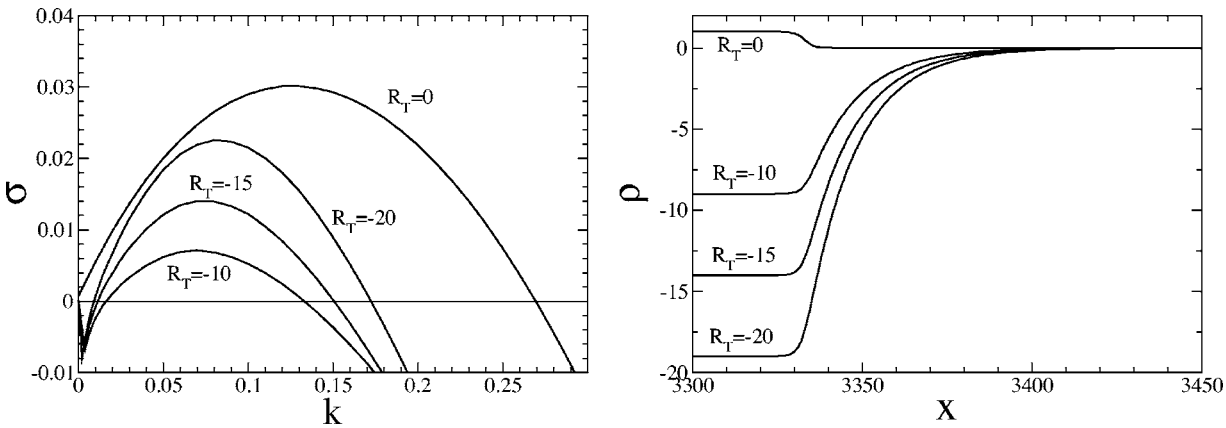


FIG. 6. Dispersion curves and density profiles as a function of $x$ in quadrant 4 ($R_T<0, R_c>0$); i.e., for an antagonistic descending exothermic front. The curves are drawn here for $\mathrm{Le}=10$, $R_c=1$ and various negative $R_T$. For these values of Le and $R_c$, the system is always unstable whatever the values of negative $R_T$ as we are beyond the stability pocket of quadrant 4 shown in Fig. 3. For $R_T=0$, the density profile is statically unstable and the front features a Rayleigh-Taylor instability. When $R_T$ is decreased, the density profiles are statically stable yet the dispersion curves feature unstable modes pointing to the influence of double-diffusive modes and to the influence of the chemically driven instability.

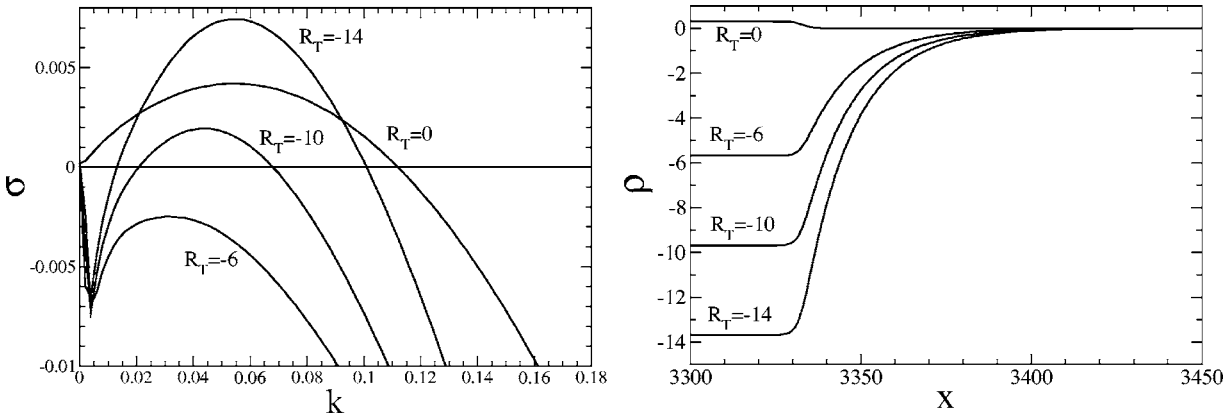


FIG. 7. Same curves as in Fig. 6, but for a smaller value of $R_c$ (=0.3) and various negative $R_T$. Here, the system is stable for intermediate values of $R_T$.

studied numerically features frozen fingers of constant amplitude and wavelength.[25,49] Figure 6 shows the dispersion curves for $R_c=1$ and decreasing negative $R_T$ for Le=10. For $R_T=0$, the Rayleigh-Taylor unstable solutal density stratification leads to a dispersion curve of type II[52] (unstable band of wave number ranging from $k=0$ up to a critical value $k_c$) and to a corresponding coarsening nonlinear dynamics. When $R_T=-10$, the density stratification is statically stable, yet the dispersion curve of type I points to the influence of double diffusion phenomena. When $R_T$ is further decreased, the system becomes even more unstable which suggests that the chemically driven instability operating in quadrant 3 is operative here too. This is confirmed by an examination of the linear stability eigenfunctions[51] which show that instability is driven ahead of the front by double diffusion and behind the front by the chemically driven instability. A small stability zone exists for $R_c$ close to zero as shown in Fig. 7 for $R_c=0.3$. There, successive transitions from Rayleigh-Taylor instability, stability, and eventually chemically driven instability is observed when $R_T$ is decreased from 0 to −6 and finally to $|R_T|<9.51$, the corresponding density profiles being statically stable for $R_T<0$.

In quadrant 2, the instability region is also largely increased when Le$>1$. Here, we have overall statically stable density profiles for $-R_c>R_T>0$ with, however, a local Rayleigh-Taylor unstable zone ahead of the front (Fig. 8). This Rayleigh-Taylor mechanism is operative ahead of the front while the chemically driven instability acts behind it, both mechanisms of instability collaborating to obtain an unstable domain in the $(R_T,R_c)$ plane much larger than for Le=1.[51] For a given negative $R_c$, dispersion curves switch then from stable curves towards type I and finally type II dispersion curves. Type I curves point to the influence of the chemically driven instability. Type II curves are obtained when $R_T$ is large enough for the strong exothermicity of the reaction to drive a Rayleigh-Bénard type of destabilization of ascending fronts. Thermal plumes are then observed as in the case of strongly exothermic ascending chlorite-tetrathionate fronts.[25,27] Oscillatory double-diffusive modes[5] have not been obtained in our analysis as they are probably overwhelmed by the chemically driven modes of instability.

## VII. CONCLUSIONS

Density differences due to changes in composition and temperature across traveling autocatalytic fronts are able to drive various buoyancy-driven instabilities that have been here classified in a parameter space ($R_T$, $R_c$) spanned by the

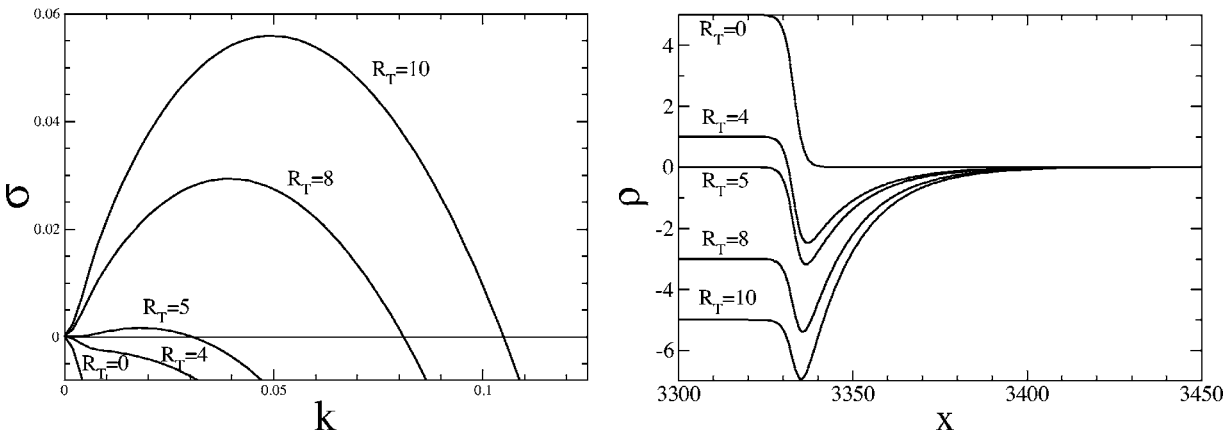


FIG. 8. Dispersion curves and density profiles as a function of $x$ in quadrant 2 for Le=10, $R_c=-5$, and various positive $R_T$. As we focus here on an ascending antagonistic exothermic front with $x$ pointing upwards against the gravity field, the density $\rho_p=-R_T-R_c$ (see Ref. 51). For isothermal systems ($R_T=0$), the reactants are solute-lighter than the products and the system is stable. It is only when $R_T$ is large enough, i.e., the products are hot enough that a destabilization takes place.

thermal and solutal Rayleigh numbers. When $R_T$ and $R_c$ are both positive, the front is unstable in the direct Rayleigh-Taylor mode because of a stratification of a solute-heavy and cold steady state lying above a solute-lighter and hotter one in the gravity field. When the Rayleigh numbers are both negative, the coupling between a localized reaction zone and differential diffusivity of mass and heat is able to destabilize the statically stable stratification of a solute-light and hot fluid above a solute-heavy and cold one. In the two other quadrants where $R_T$ and $R_c$ have opposite signs, such a counterintuitive chemically driven instability is also operative and the double-diffusive phenomena come into play as well.

Autocatalytic reactions can be classified (see Table I) as a function of the signs of the solutal $\Delta\rho_s$ and thermal $\Delta\rho_T$ density jumps across the front. As these reactions are all exothermic, i.e., $\Delta\rho_T<0$, we have, in fact, essentially two families of reactions that are the cooperative and antagonistic ones depending on whether $\Delta\rho_s$ and $\Delta\rho_T$ are both negative or have opposite signs. Positive (negative) $R_T$ correspond then to ascending (descending) fronts, while positive (negative) $R_c$ stand for the cases with $\Delta\rho_s<0$ $(>0)$.

Our classification of buoyancy-driven instabilities of exothermic fronts in the $(R_T,R_c)$ plane suggests therefore that ascending cooperative fronts feature Rayleigh-Taylor instability with dispersion curves of type II while descending cooperative fronts could be destabilized by the new chemically driven instability with dispersion curves of type I. The nonlinear dynamics is therefore expected to be quite different yielding to coarsening phenomena when ascending while featuring frozen fingers close to onset of instability when descending in the gravity field. An estimation of typical Rayleigh numbers for descending IAA fronts[50] that belong to the cooperative family gives $R_c=-3.8$ and $R_T=-3.6$, which is probably too small for the chemically driven instability to be observed. Indeed, the temperature jump across an IAA front, which is of the order of 0.5 K for typical concentrations, is quite small and heat effects are thus not dominant.[33,34] The use of a more exothermic cooperative-type reaction and the fact that experimental values of the Lewis number can be larger (up to 100) than those used here suggests however that experimental visualization of the new chemically driven instability is within experimental reach.

Isothermal antagonistic fronts like typically CT fronts are unstable due to a Rayleigh-Taylor mechanism featuring dispersion curves of type II when descending in the gravity field. When heat effects come into play, double-diffusive mechanisms as well as the new chemically driven instability can become operative for both the ascending and descending cases. Both type I and II dispersion curves can then be observed and subtle transitions between them are expected as changes in parameters are operated. It has already been demonstrated experimentally that changes in concentration can change the respective size of $\Delta\rho_c$ and $\Delta\rho_T$ for the CT system.[27] Indeed, increasing concentrations can bring the CT reaction to be exothermic enough to stabilize descending fronts and destabilize ascending ones.[27] It would be interesting to correlate such observations to the corresponding parameter values in the $(R_T,R_c)$ plane by careful measurements of the changes in $\Delta\rho_c$ and $\Delta\rho_T$ with concentrations. Further work on both cooperative and antagonistic autocatalytic reactions would help delineating the stability zones in the $(R_T, R_c)$ plane to demonstrate that the presence of chemical reactions strikingly changes the stability domain with regard to nonreactive fluids.[51]

Let us note that future experimental work aiming at testing our predicted new chemically driven instability and testing our classification of instabilities should avoid solutal double-diffusive instabilities involving two chemical species with different molecular diffusion coefficients which has been shown to allow for destabilization of descending fronts for the iodide-nitric acid[21] and iodate-sulfite[11] systems. Moreover, it is also important to ensure the use of insulating walls as thermal losses through conducting walls have been shown theoretically to also allow for destabilization of descending cooperative fronts due to the presence of nonmonotonic density profiles.[47] If the reaction is very exothermic like in combustion or for some polymerization fronts, consideration of the influence of Arrhenius dependence of the kinetic constant on temperature should be considered. Finally, let us note that the Rayleigh numbers can be varied experimentally by varying the gap width (and hence $K$), the viscosity of the solution or the composition. The large variety of autocatalytic reactions available nowadays also allow for a large pool of possible experimental conditions in which to test the classification of the different buoyancy-driven instabilities presented here.

## ACKNOWLEDGMENTS

J.D. is supported by a FRIA (Belgium) Ph.D. fellowship. A.Z. thanks the Donors of the American Chemical Society Petroleum Research Fund for support of this research. A.D. acknowledges financial support of Prodex (Belgium), of ESA, of FNRS, and of the Communauté française de Belgique ("Actions de Recherches Concertées" programme).

[1] J.-C. Micheau, M. Gimenez, P. Borckmans, and G. Dewel, Nature (London) **305**, 43 (1983).
[2] D. Avnir and M. Kagan, Nature (London) **307**, 717 (1984).
[3] G. Bazsa and I. R. Epstein, J. Phys. Chem. **89**, 3050 (1985).
[4] I. Nagypál, G. Bazsa, and I. R. Epstein, J. Am. Chem. Soc. **108**, 3635 (1986).
[5] J. A. Pojman and I. R. Epstein, J. Phys. Chem. **94**, 4966 (1990).
[6] J. A. Pojman, I. R. Epstein, T. J. McManus, and K. Showalter, J. Phys. Chem. **95**, 1299 (1991).
[7] J. A. Pojman, I. P. Nagy, and I. R. Epstein, J. Phys. Chem. **95**, 1306 (1991).
[8] J. Masere, D. A. Vasquez, B. F. Edwards, J. W. Wilder, and K. Showalter, J. Phys. Chem. **98**, 6505 (1994).
[9] J. A. Pojman, R. Craven, A. Khan, and W. West, J. Phys. Chem. **96**, 7466 (1992).
[10] I. P. Nagy and J. A. Pojman, J. Phys. Chem. **97**, 3443 (1993).
[11] A. Keresztessy, I. P. Nagy, G. Bazsa, and J. A. Pojman, J. Phys. Chem. **99**, 5379 (1995).
[12] J. A. Pojman, A. Komlósi, and I. P. Nagy, J. Phys. Chem. **100**, 16209 (1996).
[13] C. R. Chinake and R. H. Simoyi, J. Phys. Chem. **98**, 4012 (1994).
[14] B. S. Martincigh, M. J. B. Hauser, and R. H. Simoyi, Phys. Rev. E **52**, 6146 (1995).
[15] B. S. Martincigh, C. R. Chinake, T. Howes, and R. H. Simoyi, Phys. Rev. E **55**, 7299 (1997).
[16] B. S. Martincigh and R. H. Simoyi, J. Phys. Chem. A **106**, 482 (2002).
[17] M. Garbey, A. Taïk, and V. Volpert, Q. Appl. Math. **56**, 1 (1998).
[18] M. Belk, K. G. Kostarev, V. Volpert, and T. M. Yudina, J. Phys. Chem. B **107**, 10292 (2003).

[19]M. Matalon and B. J. Matkowsky, Combust. Sci. Technol. **34**, 295 (1983).
[20]N. Vladimirova and R. Rosner, Phys. Rev. E **67**, 066305 (2003).
[21]I. P. Nagy, A. Keresztessy, J. A. Pojman, G. Bazsa, and Z. Noszticzius, J. Phys. Chem. **98**, 6030 (1994).
[22]M. R. Carey, S. W. Morris, and P. Kolodner, Phys. Rev. E **53**, 6012 (1996).
[23]M. Böckmann and S. C. Müller, Phys. Rev. Lett. **85**, 2506 (2000).
[24]D. Horváth, T. Bánsági Jr., and A. Tóth, J. Chem. Phys. **117**, 4399 (2002).
[25]T. Bánsági Jr., D. Horváth, Á. Tóth, J. Yang, S. Kalliadasis, and A. De Wit, Phys. Rev. E **68**, 055301 (2003).
[26]T. Bánsági Jr., D. Horváth, and Á. Tóth, Phys. Rev. E **68**, 026303 (2003).
[27]T. Bánsági Jr., D. Horváth, and Á. Tóth, Chem. Phys. Lett. **384**, 153 (2004).
[28]T. Bánsági Jr., D. Horváth, and Á. Tóth, J. Chem. Phys. **121**, 11912 (2004).
[29]T. Rica, D. Horváth, and Á Tóth, Chem. Phys. Lett. **408**, 422 (2005).
[30]M. Böckmann and S. C. Müller, Phys. Rev. E **70**, 046302 (2004).
[31]M. C. Rogers and S. W. Morris, Phys. Rev. Lett. **95**, 024505 (2005).
[32]B. F. Edwards, J. W. Wilder, and K. Showalter, Phys. Rev. A **43**, 749 (1991).
[33]J. W. Wilder, B. F. Edwards, and D. A. Vasquez, Phys. Rev. A **45**, 2320 (1992).
[34]D. A. Vasquez, J. W. Wilder, and B. F. Edwards, J. Chem. Phys. **98**, 2138 (1993).
[35]D. A. Vasquez, J. M. Littley, J. W. Wilder, and B. F. Edwards, Phys. Rev. E **50**, 280 (1994).
[36]D. A. Vasquez, J. W. Wilder, and B. F. Edwards, J. Chem. Phys. **104**, 9926 (1996).
[37]J. Huang, D. A. Vasquez, B. F. Edwards, and P. Kolodner, Phys. Rev. E **48**, 4378 (1993).
[38]J. Huang and B. F. Edwards, Phys. Rev. E **54**, 2620 (1996).
[39]A. De Wit, Phys. Rev. Lett. **87**, 054502 (2001).
[40]J. Martin, N. Rakotomalala, D. Salin, M. Böckmann, and S. C. Müller, J. Phys. IV **11**, Pr6-99 (2001).
[41]J. Martin, N. Rakotomalala, D. Salin, and M. Böckmann, Phys. Rev. E **65**, 051605 (2002).
[42]R. Demuth and E. Meiburg, Phys. Fluids **15**, 597 (2003).
[43]J. Yang, A. D'Onofrio, S. Kalliadasis, and A. De Wit, J. Chem. Phys. **117**, 9395 (2002).
[44]D. A. Vasquez and A. De Wit, J. Chem. Phys. **121**, 935 (2004).
[45]A. De Wit, Phys. Fluids **16**, 163 (2004).
[46]D. Lima, A. D'Onofrio, and A. De Wit, J. Chem. Phys. **124**, 014509 (2006).
[47]J. D'Hernoncourt, S. Kalliadasis, and A. De Wit, J. Chem. Phys. **123**, 234503 (2005).
[48]G. Dewel, P. Borckmans, and D. Walgraef, Proc. Natl. Acad. Sci. U.S.A. **80**, 6429 (1983).
[49]S. Kalliadasis, J. Yang, and A. De Wit, Phys. Fluids **16**, 1395 (2004).
[50]J. D'Hernoncourt, A. Zebib, and A. De Wit, Phys. Rev. Lett. **96**, 154501 (2006).
[51]J. D'Hernoncourt, A. De Wit, and A. Zebib, J. Fluid Mech. (to be published).
[52]M. C. Cross and P. C. Hohenberg, Rev. Mod. Phys. **65**, 851 (1993).
[53]G. Nicolis and I. Prigogine, *Self-Organization in Nonequilibrium Systems* (Wiley, New York, 1977).
[54]*Chemical Waves and Patterns*, edited by R. Kapral and K. Showalter (Kluwer, Dordrecht, 1995).
[55]A. De Wit, Adv. Chem. Phys. **109**, 435 (1999).
[56]P. G. Baines and A. E. Gill, J. Fluid Mech. **37**, 289 (1969).
[57]J. S. Turner, in *Buoyancy Effects in Fluids* (Cambridge University Press, Cambridge, 1973).
[58]J. S. Turner, Annu. Rev. Fluid Mech. **17**, 11 (1985).
[59]D. A. Nield, Water Resour. Res. **11**, 553 (1968).
[60]D. A. Nield and A. Bejan, in *Convection in Porous Media* (Springer, Berlin, 1992).